Onset of Absolute Instability Induced by Viscous Dissipation in the Poiseuille-Darcy-Benard Convection of a Newtonian Fluid

2014 J. Phys.: Conf. Ser. 547 012039

(http://iopscience.iop.org/1742-6596/547/1/012039)

Journal of Physics: Conference Series **547** (2014) 012039 doi:10.1088/1742-6596/547/1/012039

Onset of Absolute Instability Induced by Viscous Dissipation in the Poiseuille-Darcy-Bénard Convection of a Newtonian Fluid

P. V. Brandão[1], L. S. de B. Alves[1] and A. Barletta[2]

[1]Programa de Pós-Graduação em Engenharia Mecânica, Universidade Federal Fluminense, Rua Passo da P átria 156, Bloco E, São Domingos, Niterói, RJ 24210-240, Brazil.
[2]Dipartimento di Ingegneria Industriale, Alma Mater Studiorum Università di Bologna, Viale Risorgimento 2, I-40136 Bologna, Italy.

E-mail: leonardo.alves@mec.uff.br

Abstract. The present paper investigates the transition from convective to absolute instability induced by viscous dissipation. As far as the authors are aware, this is the first time such a study is reported in the literature. Its framework is provided by the Poiseuille-Darcy-Bénard convection of a Newtonian fluid. We found the same behaviour observed in the absence of viscous dissipation whenever the Gebhart number is smaller than $Ge < 0.95$, which is the stabilising effect of the cross flow. When $0.95 < Ge < 4.31$, weak cross flows still stabilise the onset of absolute instability but stronger cross flows destabilise it. For a stronger viscous dissipation, i.e. $Ge > 4.31$, the cross flow always destabilises this onset. The latter two conditions create a scenario where viscous dissipation is capable of inducing a transition to absolute instability in the absence of wall heating, i.e. with a zero Rayleigh number.

1. Introduction

Buoyancy induced natural convection is an important phenomenon that has been widely studied over the past century. In the present paper, we focus on a special subset of this problem that takes place in a fluid-saturated porous medium. It has important applications in geophysical and engineering research and technology, including aquifers in permeable rocks, underground pollutant dispersion, solar energy collectors, and so on. A detailed discussion of many possible applications and their respective literature review can be found elsewhere [1, 2]. The onset of convection through buoyancy was first postulated more than a hundred years ago [3], although it was later found that natural convection in this particular study was induced by surface tension gradients at the interface between liquid and air [4, 5]. Applications for this phenomenon abound in the areas of film cooling, crystal growth, electronic equipment cooling in microgravity, and so on. More information about this interface tension gradient induced natural convection can also be found elsewhere [6, 7].

This classical driver for natural convection known as buoyancy works as follows: Adverse density gradients force gravity to push higher density fluid downwards against lower density fluid, which moves upwards due to mass conservation. Density gradients can be imposed by one of several traditional mechanisms, such as internal heating as well as solid boundaries with differentially prescribed temperatures and/or concentrations, including any variations where

their gradients are prescribed instead. Viscous dissipation has also been considered a possible mechanism for the generation of density gradients. Its influence on the heat transfer and fluid dynamics of the flow within a saturated a porous medium has been investigated for the first time over twenty years ago [8]. However, it took many years for this topic to be further considered by other researchers [9, 10]. It was only recently that viscous dissipation has been found responsible for mixed convection in porous media flows [11, 12]. In the presence of a strong enough through flow, viscous dissipation generates a nonuniform temperature distribution in an incompressible fluid, which, in turn, creates the necessary density gradients for buoyancy to initiate mixed convection. Several linear stability analyzes, such as the ones performed in these two former studies, have been performed since then to uncover similar onsets of mixed convection. They include porous media with lateral confinement [13], Darcy-Hadley flows [14] as well as Darcy-Bénard convection with through flow of viscoelastic fluids [15]. Similar studies have also been performed for viscous dissipation induced thermal instabilities in the Couette [16] and Poiseuille [17] flows of clear fluids.

One important drawback of the aforementioned studies is their use of a temporal stability analysis alone, which is only able to predict the onset of convective instabilities. Today it is well known that the onset of mixed convection might appear as an absolute instability instead of a convective one in the presence of through flow [18]. The onset of convective instability is determined with a temporal stability analysis, yielding the critical point beyond which a disturbance will grow in time in a reference frame that travels with the base flow. When observed from a laboratory (stationary) reference frame, it manifests as spatial growth. If the control parameter is increased beyond its first critical value, disturbances might become strong enough to overcome the base flow and travel upstream. This second critical point represents the onset of absolute instability, manifesting through the appearance of a pinching point in a spatial stability analysis, which is a saddle point formed between upstream and downstream travelling modes in the complex wave number map. The need to distinguish between spatial and temporal disturbance growth to identify the convective or absolute nature of the instability was first proposed in the context of plasma instabilities [19]. This is accomplished by analyzing the evolution and asymptotic behavior of wave packets initially subjected to an impulse excitation, which was originally done for boundary-layers [20]. A complete methodology for this analysis was soon developed for local and parallel shear flows subject to two-dimensional [21] as well as three-dimensional [22] instabilities. However, the latter is a quite nontrivial task when the dispersion relation does not have an algebraic form and there is no well established approach in the literature to deal with the numerical difficulties that arise when this is not the case [23].

The present paper is an extension of earlier work on the onset of convective instabilities in mixed convection within a fluid-saturated porous medium [11, 15]. On the one hand, the former study considered viscous dissipation as the only source of base flow temperature gradients. Furthermore, they derived an algebraic dispersion relation, but considered transverse and longitudinal rolls as separate two-dimensional disturbances. On the other hand, the latter study considered both viscous dissipation and differentially heated boundaries simultaneously as sources of base flow temperature gradients. In addition, it considered an Oldroyd-B fluid model, although a Newtonian fluid was analyzed as a limiting case. However, it derived a differential dispersion relation for three-dimensional disturbances, but solved this equation numerically. In the present paper, an algebraic dispersion relation is derived for the Newtonian fluid limiting case and used to determine its onset of absolute instability.

2. Mathematical Model

Two horizontal plane walls at $z^* = 0$ and h^* confine the fluid-saturated porous medium. They allow slip, are impermeable and maintained at uniform but different temperatures. In this configuration, x^* and y^* are the stream wise and span wise coordinates in the $\hat{\mathbf{i}}$ and $\hat{\mathbf{j}}$ directions,

respectively. According to an incompressible flow model subject to the Oberbeck-Boussinesq approximation, it is possible to write conservation of mass as

$$\nabla \cdot \mathbf{u}^* = 0 \quad , \tag{1}$$

conservation of momentum through the Darcy's law as

$$\frac{\mu^*}{\kappa^*}\,\mathbf{u}^* = \mathbf{F}^* \quad , \tag{2}$$

and conservation of energy as

$$\sigma^*\,\frac{\partial T^*}{\partial t^*} + \mathbf{u}^* \cdot \nabla T^* = \varkappa^*\,\nabla^2 T^* + \frac{\mathbf{F}^* \cdot \mathbf{u}^*}{\rho_h^*\,c^*} \quad , \tag{3}$$

where the drag force driving the flow is defined as

$$-\mathbf{F}^* = \nabla \mathcal{P}^* + \rho_h^*\,\mathbf{g}^*\,\beta^*\,(T^* - T_h^*) \quad , \tag{4}$$

and the term $\mathbf{F}^* \cdot \mathbf{u}^*$ is the thermal power per unit volume generated by viscous dissipation. In the above equations, $\mathbf{u}^*$ is the velocity vector, μ^* is the dynamic viscosity, κ^* is the permeability, t^* is the time coordinate, T^* is the temperature, ρ_h^* is the fluid density at the reference temperature T_h^*, c^* is the specific heat of the fluid, σ^* is the volumetric heat capacity of the saturated porous medium divided by $\rho_h^*\,c^*$, $\varkappa^*$ is the effective thermal difusivity, $\mathcal{P}^*$ is the gauge pressure with respect to the hydrostatic pressure, $\mathbf{g}^* = -g^*\,\hat{\mathbf{k}}$ is the gravity acceleration vector, where g^* is the gravity acceleration and $\hat{\mathbf{k}}$ is the unit vector associated with the z^* coordinate and β^* is the fluid thermal expansion coefficient.

This flow is also subject to the following boundary conditions

$$z^* = 0 \quad \rightarrow \quad w^* = 0 \quad \text{and} \quad T^* = T_0^* \quad , \tag{5}$$

$$z^* = h^* \quad \rightarrow \quad w^* = 0 \quad \text{and} \quad T^* = T_h^* \quad , \tag{6}$$

where (u^*, v^*, w^*) are the three velocity components associated with the (x^*, y^*, z^*) coordinates in the $(\hat{\mathbf{i}}, \hat{\mathbf{j}}, \hat{\mathbf{k}})$ unit vector directions of $\mathbf{u}^*$, respectively, u_0^* is a uniform stream wise velocity, T_0^* is the prescribed lower wall temperature and T_h^* the prescribed upper wall temperature.

2.1. Dimensionless Model

Equations (1) to (6) can be written in dimensionless form using

$$\mathbf{u} = \frac{\mathbf{u}^*}{\varkappa^*/h^*} \quad , \quad \mathbf{F} = \frac{\mathbf{F}^*}{(\varkappa^*\,\mu^*)/(h^*\,\kappa^*)} \quad , \quad \mathbf{x} = \frac{\mathbf{x}^*}{h^*} \quad ,$$

$$t = \frac{t^*}{\sigma^*\,(h^*)^2/\varkappa^*} \quad , \quad \mathcal{P} = \frac{\mathcal{P}^*}{\mu^*\,\varkappa^*/\kappa^*} \quad \text{and} \quad T = \frac{T^* - T_h^*}{T_0^* - T_h^*} \quad , \tag{7}$$

as the scaling, leading to the following dimensionless parameters

$$Ra = \frac{\rho_h^*\,g^*\,\beta^*\,(T_0^* - T_h^*)\,\kappa^*\,h^*}{\mu^*\,\varkappa^*} \quad , \quad Ge = \frac{g^*\,\beta^*\,h^*}{c^*} \quad \text{and} \quad Pe = \frac{u_0^*\,h^*}{\varkappa^*} \quad , \tag{8}$$

which define the Rayleigh, Gebhart and Péclet numbers, respectively. They become

$$\nabla \cdot \mathbf{u} = 0 \quad , \tag{9}$$

for mass conservation,

$$\mathbf{u} = \mathbf{F} = Ra\, T\, \hat{\mathbf{k}} - \nabla \mathcal{P} \quad , \tag{10}$$

for Darcy's law and

$$\frac{\partial T}{\partial t} + \mathbf{u} \cdot \nabla T = \nabla^2 T + \frac{Ge}{Ra}\, \mathbf{F} \cdot \mathbf{u} \quad , \tag{11}$$

for energy conservation, subject to dimensionless boundary conditions

$$z = 0 \quad \rightarrow \quad w = 0 \quad \text{and} \quad T = 1 \quad , \tag{12}$$

$$z = 1 \quad \rightarrow \quad w = 0 \quad \text{and} \quad T = 0 \quad . \tag{13}$$

2.2. Base Flow
A known steady-state of Eqs. (9) to (13) is given by

$$\mathbf{u}_b = \mathbf{F}_b = Pe\, \hat{\mathbf{i}} \quad , \quad T_b(z) = 1 - z + \frac{Ge\, Pe^2}{2\, Ra}\, (1 - z)\, z \quad \text{and}$$

$$\mathcal{P}_b(x, z) = \mathcal{P}_0 - Pe\, x + \frac{Ra}{2}\, (2 - z)\, z + \frac{Ge\, Pe^2}{12}\, (3 - 2\, z)\, z^2 \quad , \tag{14}$$

where $\mathcal{P}_0$ is a reference pressure and the subscript b means base flow, since Eq. (14) is the stationary and parallel solution whose linear stability is being investigated in the present paper.

3. Algebraic Dispersion Relation

3.1. Linear Disturbances
In order to do so, small disturbances are superposed to base flow (14) using

$$\begin{aligned} \mathbf{u}(x, y, z, t) &= \mathbf{u}_b(z) + \epsilon\, \mathbf{u}_d(x, y, z, t) \quad , \\ T(x, y, z, t) &= T_b(z) + \epsilon\, T_d(x, y, z, t) \quad \text{and} \\ \mathcal{P}(x, y, z, t) &= \mathcal{P}_b(x, z) + \epsilon\, \mathcal{P}_d(x, y, z, t) \quad , \end{aligned} \tag{15}$$

where $\mathbf{u}_d = (u_d\, , v_d\, , w_d)$, ϵ is the disturbance amplitude parameter and the subscript d means disturbance. Substituting relations (15) into Eqs. (9) to (11) leads to new systems of equations at different orders in ϵ. The base flow equations that lead to solutions (14) are recovered at order zero, i.e. by collecting all terms of $O(\epsilon^0)$, whereas the linear disturbance equations

$$\nabla \cdot \mathbf{u}_d = 0 \quad , \tag{16}$$

$$\mathbf{u}_d = \mathbf{F}_d = Ra\, T_d\, \hat{\mathbf{k}} - \nabla \mathcal{P}_d \quad , \tag{17}$$

$$\frac{\partial T_d}{\partial t} + \mathbf{u}_b \cdot \nabla T_d + \mathbf{u}_d \cdot \nabla T_b = \nabla^2 T_d + \frac{Ge}{Ra}\, (\, \mathbf{F}_b \cdot \mathbf{u}_d + \mathbf{F}_d \cdot \mathbf{u}_b\,) \quad , \tag{18}$$

for conservation of mass, momentum and energy, respectively, are found at order one, i.e. by collecting all terms of $O(\epsilon^1)$. The same can be done to boundary conditions (12) and (13), which leads to

$$z = 0 \quad \rightarrow \quad w_d = T_d = 0 \quad \text{and} \tag{19}$$

$$z = 1 \quad \rightarrow \quad w_d = T_d = 0 \quad , \tag{20}$$

for the linear disturbances.

3.2. Normal Modes

Disturbances are now assumed to have a wave like behavior in the homogeneous directions, which allows them to be decomposed as Fourier modes in the form of

$$\begin{aligned} \mathbf{u}_d(x,y,z,t) &= \hat{\mathbf{u}}(z)\,\exp[\,i\,(\alpha\,x+\beta\,y-\omega\,t)\,] \quad , \\ T_d(x,y,z,t) &= \hat{T}(z)\,\exp[\,i\,(\alpha\,x+\beta\,y-\omega\,t)\,] \quad \text{and} \\ \mathcal{P}_d(x,y,z,t) &= \hat{\mathcal{P}}(z)\,\exp[\,i\,(\alpha\,x+\beta\,y-\omega\,t)\,] \quad , \end{aligned} \tag{21}$$

where the hat symbol $\hat{}$ indicates a normal mode amplitude varying in the non-homogeneous direction and $i=\sqrt{-1}$. Substituting relations (21) into Eqs. (16) to (18) leads to

$$i\,\alpha\,\hat{u}(z)+i\,\beta\,\hat{v}(z)+\hat{w}'(z)=0 \quad , \tag{22}$$

from linear disturbance mass conservation Eq. (16),

$$i\,\alpha\,\hat{\mathcal{P}}(z)+\hat{u}(z) = 0 \quad , \tag{23}$$

$$i\,\beta\,\hat{\mathcal{P}}(z)+\hat{v}(z) = 0 \quad \text{and} \tag{24}$$

$$\hat{\mathcal{P}}'(z)+\hat{w}(z) = Ra\,\hat{T}(z) \quad , \tag{25}$$

from linear disturbance momentum conservation Eq. (17) and

$$i\,(Pe\,\alpha-\omega)\,\hat{T}(z)+T_b'(z)\,\hat{w}(z)=\hat{T}''(z)-(\alpha^2+\beta^2)\,\hat{T}(z)+2\,\frac{Ge\,Pe}{Ra}\,\hat{u}(z) \quad , \tag{26}$$

from linear disturbance energy conservation Eq. (18). Equations (22) to (26) can be combined to generate a single fourth-order ordinary differential equation for the linear disturbance cross stream velocity component, given by

$$\begin{aligned} &\hat{w}''''(z)-i\left(Pe\,\alpha-2\,i\left(\alpha^2+\beta^2\right)-\omega\right)\hat{w}''(z)-2\,i\,\alpha\,Ge\,Pe\,\hat{w}'(z)+ \\ &\left(\alpha^2+\beta^2\right)\left(i\,Pe\,\alpha+\left(\alpha^2+\beta^2\right)-i\,\omega+Ra\,T_b'(z)\right)\hat{w}(z)=0 \quad , \end{aligned} \tag{27}$$

which is subject to boundary conditions

$$z=0 \quad \rightarrow \quad \hat{w}=\hat{w}''=0 \quad \text{and} \tag{28}$$

$$z=1 \quad \rightarrow \quad \hat{w}=\hat{w}''=0 \quad , \tag{29}$$

where the impermeable wall boundary conditions are complemented by the additional zero second derivative boundary conditions, derived from the isothermal wall boundary conditions through relation

$$\hat{T}(z)=\frac{\left(\alpha^2+\beta^2\right)\hat{w}(z)-\hat{w}''(z)}{Ra\left(\alpha^2+\beta^2\right)} \quad , \tag{30}$$

obtained by combining Eqs. (22) to (25). Equations (27) to (29) are collectively known as the dispersion relation. They must be solved to identify the eigenvalues, given by α, β and ω, that characterize the present problem as functions of the governing parameters Pe, Ge and Ra.

3.3. Generalized Integral Transform Technique

The search for an absolute instability onset has a large computational time cost when it relies solely on a graphical verification of the pinching condition. However, this cost can be greatly reduced when the zero group velocity conditions can be employed beforehand to find possible saddle points. Since these conditions are necessary but not sufficient, the pinching condition still must be verified graphically. Nevertheless, it is significantly less costly to do so if the possible saddle point location is already known. Arguably the major difficulty restricting the use of this alternative approach is the differential form of the dispersion relation. Hence, the next step in the present procedure is to reduce Eqs. (27) to (29) to an algebraic form. This is achieved here through the Generalized Integral Transform Technique [24, 25], which is an extension of Separation of Variables and the Classical Integral Transform Technique [26].

In order to generate this algebraic dispersion relation, an eigensystem must be defined for the integral transformation procedure. An adequate system for the present problem can be obtained from homogeneous equation

$$\psi_m''''(z) = \lambda_m^4 \, \psi_m(z) \quad \text{with} \quad m = 1\,,\, 2\,,\, 3\,,\, \ldots\,,\, N_Z \quad , \tag{31}$$

subject to homogeneous boundary conditions

$$z = 0 \quad \rightarrow \quad \psi_m = \psi_m'' = 0 \quad \text{and} \tag{32}$$

$$z = 1 \quad \rightarrow \quad \psi_m = \psi_m'' = 0 \quad , \tag{33}$$

leading to normalized eigenfunctions

$$\tilde{\psi}_m(z) = -\frac{\sinh[\,\lambda_m\,]\,\sin[\,\lambda_m\,z\,]}{\sqrt{N_m}} \quad , \tag{34}$$

where their respective eigenvalues are defined as

$$\lambda_m = m\,\pi \quad , \tag{35}$$

and norm is defined as

$$N_m = \frac{\cos[\,2\,\lambda_m\,] + \cosh[\,2\,\lambda_m\,]}{4} - \frac{1}{2} \quad . \tag{36}$$

Having established the eigensystem to be used for the integral transformation procedure, it is now possible to define the inverse/transform pair

$$\hat{w}(z) \;=\; \sum_{m=1}^{N_Z} \tilde{w}_m \, \tilde{\psi}_m(z) \quad \text{and} \tag{37}$$

$$\tilde{w}_m \;=\; \int_0^1 \tilde{\psi}_m(z)\,\hat{w}(z)\,dz \quad , \tag{38}$$

where the integral transformed cross stream velocity component defined in Eq. (37) forms the new algebraic variable set with N_Z terms. Since eigensystem (31) to (36) belongs to the Sturm-Liuville class, the summation in Eq. (38) is convergent. Hence, N_Z can be chosen high enough to yield a solution for the eigenvalues α, β and ω with the desired user prescribed accuracy.

Substituting base flow (14) into disturbance Eq. (27), multiplying the result by normalized eigenfunction (34) and integrating it over the dimensionless domain leads to

$$\int_0^1 \tilde{\psi}_m(z)\,\hat{w}''''(z)\,dz - i\left(Pe\,\alpha - 2\,i\left(\alpha^2+\beta^2\right)-\omega\right)\int_0^1 \tilde{\psi}_m(z)\,\hat{w}''(z)\,dz\;-$$
$$2\,i\,\alpha\,Ge\,Pe\int_0^1 \tilde{\psi}_m(z)\,\hat{w}'(z)\,dz - \left(\alpha^2+\beta^2\right)Ge\,Pe^2\int_0^1 z\,\tilde{\psi}_m(z)\,\hat{w}(z)\,dz\;+ \tag{39}$$
$$\frac{1}{2}\left(\alpha^2+\beta^2\right)\left(Ge\,Pe^2+2\,i\left(Pe\,\alpha-\omega-i\left(\alpha^2+\beta^2-Ra\right)\right)\right)\int_0^1 \tilde{\psi}_m(z)\,\hat{w}(z)\,dz = 0 \quad ,$$

where the first integral can be split by parts to yield

$$\int_0^1 \tilde{\psi}_m(z)\,\hat{w}''''(z)\,dz = \int_0^1 \tilde{\psi}_m''''(z)\,\hat{w}(z)\,dz = \lambda_m^4\int_0^1 \tilde{\psi}_m(z)\,\hat{w}(z)\,dz = \lambda_m^4\,\tilde{w}_m \tag{40}$$

upon substitution of Eqs. (31) and (38). Using this result as well as inverse and transform definitions given by Eqs. (37) and (38), respectively, Eq. (39) can be re-written as

$$\sum_{n=1}^{N_Z} A_{m,n}\,\tilde{w}_n = 0 \quad , \tag{41}$$

with integral transform coefficient matrix being defined as

$$A_{m,n} = \left(\lambda_m^4 + \frac{1}{2}\left(\alpha^2+\beta^2\right)\left(Ge\,Pe^2+2\,i\left(Pe\,\alpha-\omega-i\left(\alpha^2+\beta^2-Ra\right)\right)\right)\right)A_{m,n}^{(0)} \tag{42}$$
$$-\left(\alpha^2+\beta^2\right)Ge\,Pe^2\,A_{m,n}^{(1)} - 2\,i\,\alpha\,Ge\,Pe\,A_{m,n}^{(2)} - i\left(Pe\,\alpha-2\,i\left(\alpha^2+\beta^2\right)-\omega\right)A_{m,n}^{(3)}$$

which is itself dependent on eigenfunction integral coefficients

$$A_{m,n}^{(0)} = \int_0^1 \tilde{\psi}_m(z)\,\tilde{\psi}_n(z)\,dz = \delta_{m,n} \quad , \tag{43}$$

$$A_{m,n}^{(1)} = \int_0^1 z\,\tilde{\psi}_m(z)\,\tilde{\psi}_n(z)\,dz \quad , \tag{44}$$

$$A_{m,n}^{(2)} = \int_0^1 \tilde{\psi}_m(z)\,\tilde{\psi}_n'(z)\,dz \quad \text{and} \tag{45}$$

$$A_{m,n}^{(3)} = \int_0^1 \tilde{\psi}_m(z)\,\tilde{\psi}_n''(z)\,dz \quad , \tag{46}$$

where $\delta_{m,n}$ is the Kronecker delta and the remaining coefficients yield analytical expressions.

Equation (41) will only have a nontrivial solution when

$$\det[\,A_{m,n}\,] = 0 \quad , \tag{47}$$

for a fixed value of N_Z, which is the final form of the algebraic dispersion relation. A possible onset of absolute instability is then identified using the zero group velocity conditions

$$\frac{\partial \det[\,A_{m,n}\,]}{\partial\alpha} = 0 \quad \text{with} \quad \frac{\partial\omega}{\partial\alpha} = 0 \quad \text{and} \quad \frac{\partial \det[\,A_{m,n}\,]}{\partial\beta} = 0 \quad \text{with} \quad \frac{\partial\omega}{\partial\beta} = 0 \quad , \tag{48}$$

as additional equations in the system of three equations for the three unknowns α_A, β_A and ω_A, which identify a possible saddle point location. Its behavior is then analyzed graphically to verify if it satisfies the pinching condition, confirming it as an onset of absolute instability.

4. Results and Discussion

4.1. Single Term Approximation

It is useful to first investigate an approximate solution of Eqs. (47) and (48) when the symmetric matrix (42) is generated with $N_Z = 1$ term only. In this case, Eq. (47) yields

$$\pi^4 + \pi^2(i\,Pe\,\alpha + 2\,(\alpha^2+\beta^2) - i\,\omega) + (\alpha^2+\beta^2)(i\,Pe\,\alpha + \alpha^2 + \beta^2 - i\,\omega - Ra) = 0 \quad , \tag{49}$$

while the zero group velocity conditions in Eq. (48) yield

$$i\,Pe\,(\,\pi^2 + 3\,\alpha^2 + \beta^2\,) + 2\,\alpha\,(\,2\,\pi^2 + 2\,(\,\alpha^2+\beta^2\,) - i\,\omega - Ra\,) \;=\; 0 \quad \text{and} \tag{50}$$

$$\beta\,(\,2\,\pi^2 + i\,Pe\,\alpha + 2\,(\,\alpha^2+\beta^2\,) - i\,\omega - Ra\,) \;=\; 0 \quad , \tag{51}$$

respectively. Two important conclusions can be drawn from these simplified relations. The first one is their Gebhart number independence of Eq. (49) and, hence, Eqs. (50) and (51) as well, i.e. the transition to absolute instability does not vary with Gebhart when $N_Z = 1$. Since the above relations are expected to be increasingly more accurate as the Gebhart number decreases, such a conclusion is not entirely unexpected as it is true as well for the onset of convective instability. The second conclusion is the existence of an onset of absolute instability for transverse modes, which arises from the fact that $\beta = 0$ is an obvious solution of Eq. (51). In fact, we were not able to find an onset of absolute instability for either oblique modes or longitudinal modes, independent of the value of N_Z utilize.

4.2. Convergence Analysis

A convergence study for the onset of absolute instability has been performed and shown in Fig. 1, which presents the critical Rayleigh number relative error as a function of the Péclet number with $Ge = 5$. This particular case was selected because it was the highest Gebhart number studied and convergence worsens when this parameter is increased. Furthermore, the error for each solution generated with N_Z terms was estimated using the solution generated with $N_Z + 1$ terms. It is clear in this figure that graphically converged curves can be obtained using $N_Z = 5$ terms in the summation series, since maximum relative errors are smaller than 1%. Hence, all results presented next were obtained with this number of terms. Furthermore, only transverse modes are shown in the present paper for the reason discussed in the previous subsection.

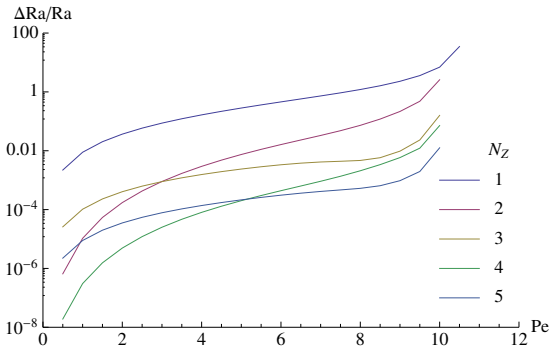

Figure 1. Relative error of the critical Rayleigh number for the onset of absolute instability with $Ge = 5$ as a function of Pe for different N_Z.

4.3. Numerical Solution

Figures 2 shows both onsets of convective and absolute instability, through the critical Rayleigh number and frequency, for transverse modes as functions of the Pe with $Ge = 0.01$, 0.1, 1, 2 and 5. When $Ge = 0.01$, both onsets agree with reported data in the literature for the case without viscous dissipation within the reported Péclet range [27]. In this limiting scenario, the onset of convective instability is not affected by the cross flow whereas the onset of absolute instability is always stabilized by it. When viscous dissipations is present, the cross flow always destabilises the onset of convective instability. Furthermore, this effect gets stronger as the Gebhart number increases. On the other hand, this scenario changes at the transition to absolute instability. Cross flow destabilisation is only observed for weak viscous dissipation. Beyond a certain threshold, estimated here to be $Ge_{c_1} \simeq 0.95$, weak cross flows stabilise the onset of absolute instability but stronger cross flows destabilise this onset. In addition, beyond a second threshold, estimated here to be $Ge_{c_1} \simeq 4.31$, the cross flow is always a destabilising factor for the onset of absolute instability. This behaviour leads to the peculiar condition where a transition to absolute instability can be observed even without a temperature difference between horizontal walls, i.e. even when $Ra = 0$. Finally, these transverse modes are always oscillatory in the presence of cross flow. Although their frequency does not vary significantly with the Gebhart number for weak cross flows, an increase in this parameter increases the critical frequency associated with both onsets for strong cross flows.

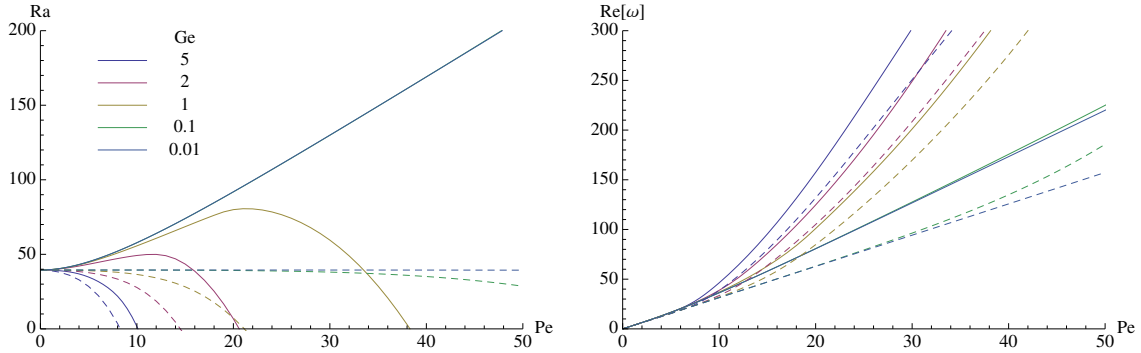

Figure 2. Critical Rayleigh number (left) and frequency (right) for the onsets of convective (dashed lines) and absolute (solid lines) instability as a function of Pe for different Ge.

All results presented so far were obtained using the zero group velocity conditions in Eqs (48), in addition to the dispersion relation (47). However, these conditions are necessary but not sufficient for the determination of an onset of absolute instability. In order to prove they indeed represent such an onset, a graphical analysis of the saddle point formation is required, showing a merger between originally upstream and downstream propagating modes. Figure 3 presents this analysis for $Pe = 30$ and $Ge = 1$, showing the simultaneous pinching of the saddle point $\alpha = 4.86559 - 5.86233\,i$ and $\beta = 0$ in both complex wave number maps. A few other points were similarly analysed and the same behaviour was observed. Hence, we expect this to be the case for all data points shown in Fig. 2.

5. Conclusions

The present paper considered the effects of viscous dissipation on the onset of absolute instability for a Newtonian fluid flowing inside a porous medium subjected to differentially heated horizontal walls. Three different regimes were identified. The first one is the small viscous dissipation regime, where the zero viscous dissipation behaviour is observed. On the other hand, the second regime is the average viscous dissipation one, where weak cross flows stabilise this onset but

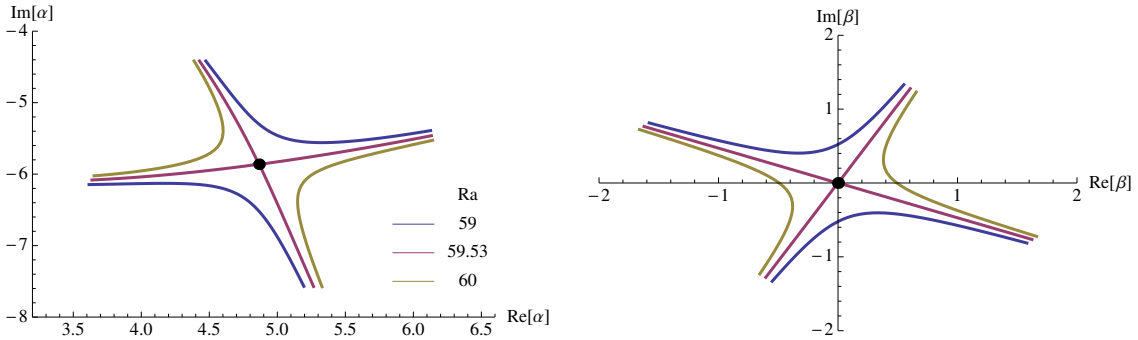

Figure 3. Simultaneous pinching point in stream wise (left) and transverse (right) complex wave number maps. Black dot indicates the saddle point located at $\alpha = 4.86559 - 5.86233\,i$, $\beta = 0$, $Ra = 59.5294$ and $\omega = 201.085$ for $Pe = 30$ and $Ge = 1$.

strong cross flows destabilise it. Finally, the cross flow always destabilises this onset in the third regime with strong viscous dissipation.

Additional studies will be pursued to verify the existence of additional transversal modes and well as the non existence of longitudinal or oblique modes. Furthermore, disturbance stream function behaviour will be investigated for positive and negative Rayleigh numbers. These studies will also include an extension to non-Newtonian fluids.

References

[1] Kaviany M 1995 *Principles of Heat Transfer in Porous Media* 2nd ed (New York: Springer – Verlag)
[2] Nield D A and Bejan A 2006 *Convection in Porous Media* 3rd ed (New York: Springer)
[3] Bénard H 1900 *Rev. Gén. Sci. Pures Appl.* **12** 1261–1309
[4] Block M 1956 *Nature* **178** 650
[5] Pearson J R A 1958 *Journal of Fluid Mechanics* **4** 489–500
[6] Simanovskii I B and Nepomnyashchy A A 1993 *Convective Instabilities in Systems with Interface* (Amsterdam: Gordon and Breach Science Publishers S.A.)
[7] Nepomnyashchy A A, Velarde M G and Colinet P 2001 *Interfacial Phenomena and Convection* (*Monographs and Surveys in Pure and Applied Mathematics* vol 124) (Boca Raton: Chapman & Hall/CRC)
[8] Nakayama A and Pop I 1989 *International Communications in Heat & Mass Transfer* **16** 173–180
[9] Murthy P V S N 1998 *Heat and Mass Transfer* **33** 295–300
[10] Nield D A 2000 *Transport in Porous Media* **41** 349–357
[11] Barletta A, Celli M and Rees D A S 2009 *International Journal of Heat and Mass Transfer* **52** 337–344
[12] Barletta A and Rees D A S 2009 *International Journal of Heat and Mass Transfer* **52** 2300–2310
[13] Barletta A and Storesletten L 2010 *International Journal of Thermal Sciences* **49** 621–630
[14] Barletta A and Rees D A S 2012 *Physics of Fluids* **24** 22
[15] de B Alves L S, Barletta A, Hirata S and Ouarzazi M N 2014 *International Journal of Heat and Mass Transfer* **70** 586–598
[16] Barletta A and Nield D A 2010 *Journal of Fluid Mechanics* **662** 475–492
[17] Barletta A, Celli M and Nield D A 2011 *Journal of Fluid Mechanics* **681** 499–514
[18] Huerre P and Monkewitz P A 1990 *Annual Review of Fluid Mechanics* **22** 473–537
[19] Briggs R J 1964 Electron-stream interaction with plasmas Research Monograph 29 MIT
[20] Gaster M 1968 *Physics of Fluids* **11** 723–727
[21] Huerre P and Monkewitz P A 1985 *Journal of Fluid Mechanics* **159** 151–168
[22] Brevdo L 1991 *Journal of Applied Mathematics and Physics* **42** 911–942
[23] Suslov S A 2006 *Journal of Computational Physics* **212** 188–217
[24] Cotta R M 1993 *Integral Transforms in Computational Heat and Fluid Flow* (Boca Raton, FL: CRC Press)
[25] Cotta R M (ed) 1998 *The Integral Transform Method in Thermal and Fluids Science and Engineering* (New York: Begell House, Inc.)
[26] Özisik M N 1993 *Heat Conduction* 2nd ed (New York: Wiley Interscience)
[27] Hirata S C and Ouarzazi M N 2010 *Physics Letters, Section A: General, Atomic and Solid State Physics* **374** 2661–2666